IJCRT.ORG ISSN : 2320-2882

INTERNATIONAL JOURNAL OF CREATIVE RESEARCH THOUGHTS (IJCRT)

An International Open Access, Peer-reviewed, Refereed Journal

FINITE ELEMENT MODELING OF LOW VELOCITY IMPACT INDUCED DAMAGE ANALYSIS ON FIBER REINFORCED POLYMERIC COMPOSITE STRUCTURES

[1]Semayat Fanta Herano,[2]P.M.Mohite,[3]C.S Upadhyay

[1]PhD Scholar,[2]Proffessor,[3]Proffessor

[1]Indian institute of technology Kanpur,

[1]Aerospace Engineering department, Kanpur, India

***Abstract*:** The study on low velocity impact damage in fiber reinforced laminated composite structures has a major importance in Aerospace industries. This paper deals with the development of finite element models to simulate the damage or failure initiation and its propagation in a carbon fiber reinforced polymeric matrix composite structure due to a low velocity impact. An experimental work have been conducted by authors specified in literature for a circular plate made from carbon/epoxy material which is subjected to low energy impact of different magnitude as 7.33 J, 11.03 J and 14.67 J based on a drop weight impact test according to ASTM D7136 M-15. An equivalent model is simulated using ABAQUS/Explicit finite element modeling tool using three dimensional (3D) Hashin failure criteria for intralaminar damage initiation and stiffness degradation is achieved using scalar damage variables. A three dimensional solid interface element (or cohesive element) is introduced in between adjacent layers with different fiber orientation to simulate the interlaminar damage initiation using quadratic stress criteria and Benzeggagh-Kenane (B-K) fracture criterion for damage propagation. The 3D Hashin failure criteria is implemented as the user implemented material subroutine (VUMAT) code using Fortran programming language. The damage in fiber and matrix is represented using four scalar damage variables of a particular modes of failure with the help of solution dependent state variables (SDV). The interlaminar damage is represented using the area of deleted elements of solid interface. The numerical result is validated with an experimentally obtained one from literature and showing an excellent agreement and thus it shows the accuracy of the currently proposed finite element model.

Keywords: **Damage, Finite element method, Laminated structure, , low velocity impact**

I. INTRODUCTION

Fiber reinforced polymeric composite (FRPC) materials are widely used in a wide range of structural applications in aerospace industry. The low weight combined with better specific properties such as specific strength and specific stiffness (i.e. compare to the conventional structural materials such as steel, aluminum and others) and working under wide range of temperature makes it preferable for aerospace structures such as wings, tails, propellers, rotors and fuselage. Despite of the attractive properties, the use of composite materials often restricted due to their susceptibility to barely visible damage (BVD) due to transverse impact load, leading to the necessity of a higher safety factor resulting in an increase of the total weight.

The impact response of composites has been investigated in depth in past four decades especially by experimental, and analytical formulation (Zhou 1998; Naik NK 2000; Olsson 2001; Olsson 2006; Abrate 2001; Gong SW 1994; Gong SW 1995). The analytical methods are based on mathematical and physical principles and provide a better understanding of the controlling factors but are unsuitable for predicting the impact induced damages. Experimental studies are fundamental for the verification of the theoretical and numerical predictions but are very expensive and time consuming when the experimental parameters varied over a wide range. Thus finite element methods (FE) can be used to simulate the impact event in composites using newly invented computational tools.

In this paper, numerical (FE) studies are conducted on damage and failure behavior of a laminated unidirectional carbon/epoxy composite subjected to low velocity impact. Multiple damage mechanisms are included using damage variables with Hashin three dimensional (3D) failure criteria and the stiffness degradation controlled by the scalar damage variables for the damage evolution. The modified Hashin 3D failure criteria with Puck criterion for matrix compression are applied to ABAQUS/Explicit FE tool via a user-defined material subroutine (VUMAT) to investigate the damage in fiber and matrix material that result from impact.

The intralaminar damages have been evaluated using Hashin failure criteria for fiber tension, fiber compression and matrix tension while Puck criterion (Puck and Schürmann 2001) for matrix compressive failure. For the intralaminar damage initiation 3D Hashin failure criterion (Hashin 1980) for fiber and matrix failure in both tension and compression with the Puck criteria are implemented by user subroutine (VUMAT) which is written in Fortran programming language.

II. CLASSIFICATION OF DAMAGE INDUCED DUE TO LOW VELOCITY IMPACT

The damage induced due to low velocity impact can be divided in two major categories. These are intralaminar damages and interlaminar damage. Intralaminar damage includes fiber breaking or rapture, matrix cracking, fiber/matrix debonding and fiber buckling while the interlaminar damage include the delamination between adjacent plies with different orientation. This work mainly focuses on the study of primary damage events such as fiber and matrix damage in both tension and compression modes and an interface damage that occur during low energy impact. These damages are difficult to detect with visual inspection on an impacted structural surface and are insides, thus they are called as barely visible internal damages (BVID) but still deserve high attention due to the reduction of the resultant residual compressive strength. An interface damage is also studied or simulated using a 3D interface element or cohesive element placed in between plies with different orientation.

III. MATERIAL MODEL AND FAILURE CRITERIA

The laminated FRPC are made by stacking several unidirectional layers as shown in figure (1). Because of the effect of the fiber, each laminate layer has relatively high strength and stiffness in the direction of fiber but low strength in the transverse directions. With a properly chosen matrix material, manufacturing technique and stacking sequence; optimum in-plane mechanical properties can be obtained. However, an out-of-plane load, such as impact, can cause a wide range of internal matrix micro-cracks in matrix material, which results in a low impact resistance of composite laminates; while, the microcracks propagation in the interface can lead to delaminations.

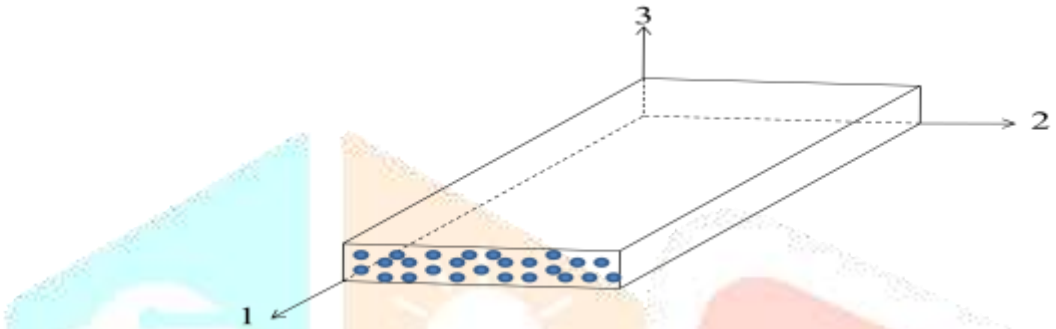

Figure 1 Principal material coordinates of layer

A. Three Dimensional Constitutive Model for Undamaged Material

The built-in damage model in ABAQUS/Explicit can be used with elements that have a plane stress formulation, that is; plane stress, membrane, and shell elements. User-defined material subroutines (VUMAT), written in Fortran language are available to extend this capability to elements with 3D stress states. In 3D, the strain-stress relations for a typical linear elastic orthotropic material implemented within ABAQUS/Explicit is with the use of UMAT or VUMAT code. The primary assumption is that elastic stress-strain relations are given by orthotropic damaged elasticity for un damaged ply is given as

$$\{\sigma\} = [C]\{\varepsilon\} \tag{1}$$

Therefore, form 3D stress-strain relation for undamaged material Equation 1 is rewritten as

$$\begin{Bmatrix} \sigma_{11} \\ \sigma_{22} \\ \sigma_{33} \\ \sigma_{23} \\ \sigma_{31} \\ \sigma_{12} \end{Bmatrix} = \begin{bmatrix} C_{11} & C_{12} & C_{13} & 0 & 0 & 0 \\ C_{12} & C_{22} & C_{23} & 0 & 0 & 0 \\ C_{13} & C_{23} & C_{33} & 0 & 0 & 0 \\ 0 & 0 & 0 & C_{44} & 0 & 0 \\ 0 & 0 & 0 & 0 & C_{55} & 0 \\ 0 & 0 & 0 & 0 & 0 & C_{66} \end{bmatrix} \begin{Bmatrix} \varepsilon_{11} \\ \varepsilon_{22} \\ \varepsilon_{33} \\ \varepsilon_{23} \\ \varepsilon_{31} \\ \varepsilon_{12} \end{Bmatrix} \tag{2}$$

Where the stiffness coefficients C_{ij} are defined in terms of the elastic material constants as

$$C_{11} = \frac{1-\nu_{23}\nu_{32}}{E_2E_3\Delta}; C_{22} = \frac{1-\nu_{13}\nu_{31}}{E_1E_3\Delta}; C_{33} = \frac{1-\nu_{12}\nu_{21}}{E_1E_2\Delta}$$

$$C_{12} = \frac{\nu_{12}+\nu_{23}\nu_{13}}{E_1E_3\Delta}; C_{13} = \frac{\nu_{13}+\nu_{23}\nu_{12}}{E_1E_2\Delta}; C_{23} = \frac{\nu_{23}+\nu_{21}\nu_{13}}{E_1E_2\Delta}; \tag{3}$$

$$C_{44} = 2G_{23}; C_{55} = 2G_{13}; C_{66} = 2G_{23}$$

where Δ is given as

$$\Delta = \frac{1-\nu_{12}\nu_{21}-\nu_{13}\nu_{31}-\nu_{23}\nu_{32}-2\nu_{21}\nu_{31}\nu_{32}}{E_1E_2E_3} \tag{4}$$

The principal direction properties of material are related as

$$\frac{\nu_{ij}}{E_i} = \frac{\nu_{ji}}{E_j} \quad i, j = 1,2,3 \tag{5}$$

where E_1, E_2 and E_3 are young's modulus of material in directions 1, 2, and 3 respectively as in Fig.(1), G_{12}, G_{13} and G_{23} are the shear modulus in the three principal directions and ν_{ij} is the poison's ratio for transverse strain in the j direction when stressed in the i direction.

B. Three Dimensional Failure Criteria for Damage Initiation

In the present work, low velocity impact events have been considered; with no perforation of the target plate by the projected impactor. The impact damage starts with localized matrix cracking called matrix microcracking that acts as an initiation point of damage of matrix and further damaging leads to delamination. Delamination occurs at the interface between plies with different orientation and is introduced by interlaminar shear stresses which are promoted due to different reasons, such as matrix cracking, difference in stiffness between the adjacent plies, and deflection of the structure. The usual shape is an oblong peanut with the major axis oriented in the fiber direction of the lower layer (S.Abrate 1998; Davies 2004). The peanut shape is a result of the shear stress distribution around the impactor, the interlaminar shear strength along the fiber direction and the matrix cracking.

The Hashin's criteria were originally developed as failure criteria for unidirectional polymeric composites, and hence, application to other laminate types or non-polymeric composites represents a significant approximation. Failure indices for the Hashin criteria are related to fiber and matrix failures and involve four failure modes. Additional failure indices result from extending the Hashin criteria to three-dimensional problems wherein the extensions are Puck criteria for the transverse compressive stress components. The failure modes included with the Hashin and Puck criteria for 3-D is given as

1. Fiber failure under tension: ($\sigma_{11} > 0$)

$$F_f^t = \left(\frac{\sigma_{11}}{X_T}\right)^2 + \left(\frac{\tau_{12}}{S_{12}}\right)^2 + \left(\frac{\tau_{13}}{S_{13}}\right)^2 \tag{6}$$

2. Fiber failure under compression: ($\sigma_{11} < 0$)

$$F_f^c = \left(\frac{\langle \sigma_{11} \rangle}{X_C}\right)^2 \tag{7}$$

3. Matrix failure under tension: ($\sigma_{22}+\sigma_{33} > 0$):

$$F_m^t = \left(\frac{\sigma_{22}+\sigma_{33}}{Y_T}\right)^2 + \frac{\tau_{23}^2 - \sigma_{33}\sigma_{33}}{S_{23}^2} + \left(\frac{\tau_{12}}{S_{12}}\right)^2 + \left(\frac{\tau_{13}}{S_{13}}\right)^2 \tag{8}$$

4. Matrix failure under compression: ($\sigma_{22}+\sigma_{33} < 0$):

$$F_m^c = \left[\left(\frac{Y_C}{2S_{23}}\right)^2 - 1\right]\frac{(\sigma_{22}+\sigma_{33})}{Y_C} + \frac{(\sigma_{22}+\sigma_{33})^2}{4S_{23}^2} + \frac{\tau_{23}^2 - \sigma_{33}\sigma_{33}}{S_{23}^2} + \left(\frac{\tau_{12}}{S_{12}}\right)^2 + \left(\frac{\tau_{13}}{S_{13}}\right)^2 \tag{9}$$

Where, the lamina strength allowable values for tension and compression in the lamina principal material directions as well as the in-plane shear strength allowable value are denoted by X_t, X_c, Y_t, Y_c, and S_{12}, respectively, Z_t and Z_c are the through-the-thickness normal strength allowable values in tension and compression, respectively, and S_{13} and S_{23} are the transverse shear strength allowable values. In eq. (1-4), the in-plane normal and shear stress components are denoted by $\sigma_{ij}(i,j=1,2,3)$. The failure indices If any failure index F_i^j exceeds unity, then failure initiation occur and material degradation will be performed. The subscript "i" implies the material indicator, that is, fiber or matrix and the superscript "j" implies the type of damage or failure in the material, that is, tensile or compressive. The failure index can be clearly be given in terms of damage variables (d_i^j) for instance

$$F_i^j = \begin{cases} d_i^j \geq 1; & \text{Fiber/matrix damage in tension/compresion} \\ d_i^j < 1; & \text{no fiber/matrix damage in tension/compresion} \end{cases} \tag{10}$$

C. Damage Evolution

Once the damage initiation criterion of Hashin and Puck is satisfied for intralaminar damage, the damage development in a laminate requires a damage evolution law. The damage evolution is characterized by stiffness reduction of the material. To compute the damaged stiffness of material, four damage variables are introduced. Two associated with fiber tension and compression d_f^t and d_f^c, and two associated with matrix tension and compression d_m^t and d_m^c, respectively. The ply dominated elastic stiffness C_{ij} is modified by the damage functions $\left(1-d_i^j\right)$, during loading to failure. Four scalar damage variables given above are introduced, having the range 0 (no damage) to 1 (fully damaged) to describe damage development in the material. Therefore the damaged stiffness matrix C_{ij}^d is given as

$$C_{ij}^{d}=\begin{bmatrix} C_{11}^{d} & C_{12}^{d} & C_{13}^{d} & 0 & 0 & 0 \\ C_{12}^{d} & C_{22}^{d} & C_{23}^{d} & 0 & 0 & 0 \\ C_{13}^{d} & C_{23}^{d} & C_{33}^{d} & 0 & 0 & 0 \\ 0 & 0 & 0 & C_{44}^{d} & 0 & 0 \\ 0 & 0 & 0 & 0 & C_{55}^{d} & 0 \\ 0 & 0 & 0 & 0 & 0 & C_{66}^{d} \end{bmatrix} \tag{11}$$

Where the damaged elastic constants (9 constants) of C_{ij}^{d}) are defined in terms of the undamaged elastic constants and the four damage variables as

$$\begin{aligned} C_{11}^{d} &= (1-d_f)C_{11} \\ C_{22}^{d} &= (1-d_f)(1-d_m^t)(1-d_m^c)C_{22} \\ C_{33}^{d} &= (1-d_f)(1-d_m^t)(1-d_m^c)C_{33} \\ C_{12}^{d} &= (1-d_f)(1-d_m^t)(1-d_m^c)C_{12} \\ C_{13}^{d} &= (1-d_f)(1-d_m^t)(1-d_m^c)C_{13} \\ C_{23}^{d} &= (1-d_f)(1-d_m^t)(1-d_m^c)C_{23} \\ C_{44}^{d} &= (1-d_f)(1-S_m^t d_m^t)(1-S_m^c d_m^c)G_{23} \\ C_{55}^{d} &= (1-d_f)(1-S_m^t d_m^t)(1-S_m^c d_m^c)G_{13} \\ C_{66}^{d} &= (1-d_f)(1-S_m^t d_m^t)(1-S_m^c d_m^c)G_{12} \end{aligned} \tag{12}$$

Where $d_f = 1-(1-d_f^t)(1-d_f^c)$, S_m^t and S_m^c, are parameters to consider matrix shear effect in tension and compression.

IV. INTERLAMINAR DAMAGE MODEL

The interface between adjacent plies of different orientation is created as a solid 3D thin layer called interface element, for simulating interlaminar or interface delamination failure.

A. Interface Damage Initiation

The damage initiation criterion of interface is usually based on stresses or strains. In this work damage is assumed to initiate when a quadratic interaction function involving the nominal stress ratios reaches a value of one[17].

$$\left(\frac{\langle \sigma_n \rangle}{N_{\max}}\right)^2+\left(\frac{\sigma_t}{T_{\max}}\right)^2+\left(\frac{\sigma_s}{S_{\max}}\right)^2=1 \tag{13}$$

Where σ_n, σ_t and σ_s represents normal and shear stresses and N_{max}, T_{max} and S_{max} denotes the interface tensile and shear strengths respectively and $\langle . \rangle$ represents the Macaulay bracket to differentiate tensile and compressive. Therefore, Macaulay brackets are used to signify that a pure compressive deformation or stress state does not initiate damage.

B. Interface damage evolution

The damage propagation criterion are used to describe the rate at which the interface material stiffness is degraded once the corresponding quadratic initiation criterion given in Equation (8) is satisfied. Among various criteria developed in the framework of common mixed-mode fracture toughness, the Benzegag and Kenan (B-K) criterion appears to be the most popular one. For this work we applied the Modified B-K criteria as [20]

$$\frac{G_{Tc}}{G_{Ic}+(G_{IIc}-G_{Ic})\left(\frac{G_{II}+G_{III}}{G_T}\right)^{\eta}} \geq 1 \tag{14}$$

Where $G_{Tc}=G_I+G_{II}+G_{III}$ the total strain energy release rate and G_I, G_{II} and G_{III} are strain energy release rate parameters in mode I and Mode II respectively. G_{Ic}, G_{IIc} are the critical values of strain energy release rate, that is, the fracture toughness of material. The fracture failure modes are as given in Figure 1 given below. The values of the critical strain energy release rate of different carbon/epoxy material are given in table 2.

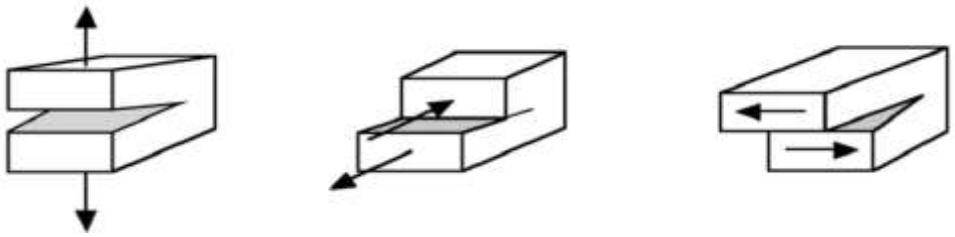

Mode I (opening) Mode II (sliding shear) Mode III (tearing shear)

Figure 1. Pure Mode Loadings[19].

V. FINITE ELEMENT MODEL

The finite element package ABAQUS/Explicit is employed to model the part and for the damage due to low velocity impact. The finite element model is based on the available experimental data given in Ref [13]. The damage initiation and evolution of intralaminar damage of cross ply laminate is implemented by a user defined material subroutine VUMAT with Fortran code. The composite laminate of size 75 mm diameter and thickness 2.0 mm consist of eight layers with each 0.25 mm of a stacking sequence $[0/90/0/90]_s$. The eight node solid elements (C3D8R) with reduced integration is used to discretize each layer. For ensuring the computational accuracy and efficiency, fine mesh with element size of 0.5 mm by 0.5 mm is employed at the impact zone while coarse mesh of 1.0 mm by 1.0 mm is utilized outside the impact region.

To simulate the delamination under low velocity impact, a ply of 10µm cohesive elements (COH3D8) are introduced in between the adjacent layers of different orientation. The failed cohesive elements are allowed to removed or delete from the model to determine the size of delamination between layers and to have stable simulation. The cohesive elements and the solid elements are connected using surface contact algorithm with the help of tie constraint to guarantee the continuity of displacement.

The plate and impactor are in general contact algorithm with normal behavior of hard contact with allowing separation after contact and tangential behavior of penalty friction coefficient of 0.3. The hemispherical shaped cylindrical impactor with diameter 16 mm is modeled as a rigid body with reference point for assigning mass and velocity, allowing for quit small deformation.

The initial velocities of impactor are varying as 2.164 m/s, 2.65 m/s and 3.06 m/s given along z-direction and concentrated masses of 3.132 kg kg is assigned to the center of mass given as reference point of the rigid impactor, resulting in different impact energies as 7.33 J, 11.03 J and 14.67 J. Before contact, the distance between the external surface of the impactor and front face of the top laminate set to nearly zero. A fixed boundary conditions are applied to composite laminate with constraining all degree of freedoms to replicate the experimental conditions. To prevent sever convergence difficulties due to element deletion the damage variables d_f and d_m may be degraded up to 0.998 rather than 1, which avoides a singularity problem of analysis.

Table 1: The fracture energy for different material are studied in [19] are given as

Carbon/epoxy materials	B-K Criteria			Power low criteria			
	G_{Ic} (kJ/m^2)	G_{Ic} (KJ/m^2)	η	G_{Ic} (kJ/m^2)	G_{Ic} (KJ/m^2)	α	β
UD carbon/epoxy	0.60	2.10	1.45	0.60	2.10	1.00	1.00
T700/M21	0.60	1.60	1.45	-0.60	1.50	1.00	1.00
AS4/3501-6	0.0816	0.554	1.75	0.103	0.648	0.17	4.80
IM7/E7T1	0.161	2.05	2.35	0.244	1.98	6.00	6.00
IM7/977-2	0.306	1.68	1.39	0.379	1.70	0.49	3.90
AS4/PEEK	0.949	1.35	0.63	0.948	1.273	2.10	0.62

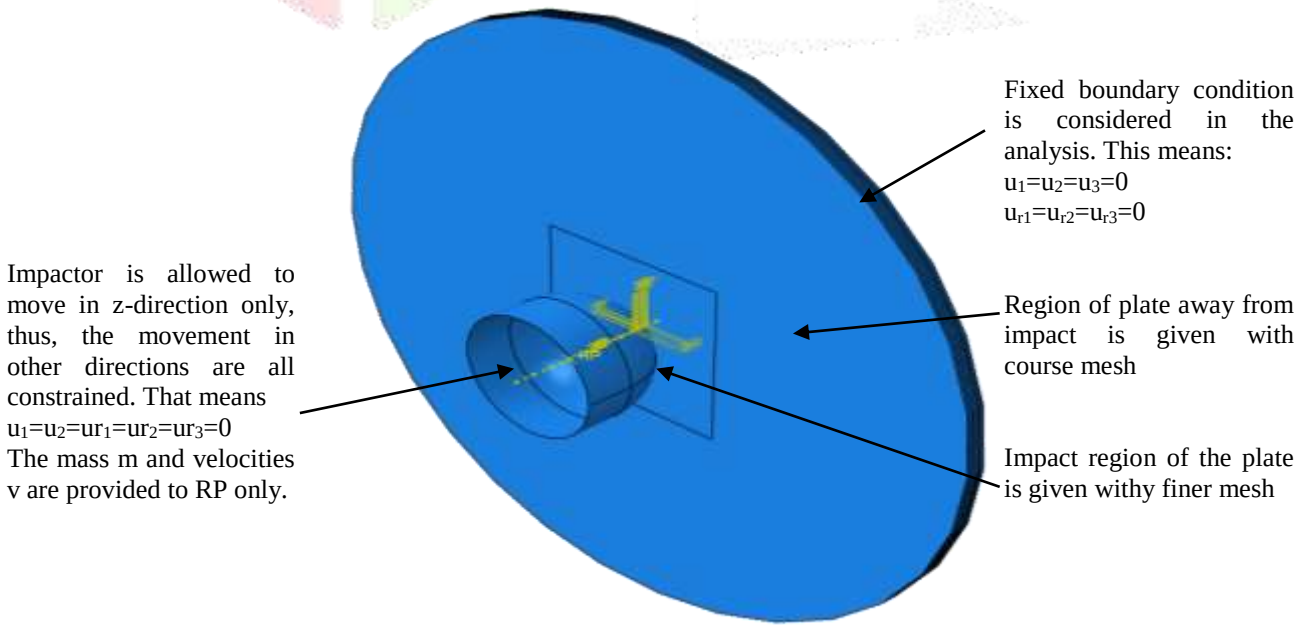

Figure 2: Finite element model, geometry and Boundry condition

The material properties of unidirectional composite and interface cohesive elements used in the simulation are cited from [18]

Table2: Material properties of the carbon fibre/epoxy unidirectional laminate used in this analysis [14],[18].

Material elastic constants (GPa)	Material Strength (MPa)	Interface properties
E_{11}= 153	X_t=2537	$K_n=K_t=K_s=2x10^5$ N/mm^3
E_{22}= 10.3	X_c=1580	N = S = T = 30 MPa
E_{33}= 10.3	Y_t = 82	G_{IC} = 0.60 N/mm
ν_{12} = 0.30	Y_c = 236	$G_{IIC} = G_{IIIC}$ =2.10 N/mm
ν_{13} = 0.30	Z_t = 82	η =1.45 (assumed)
ν_{23} = 0.40	Zc= 236	$G_{Ic}^{T} = 91.6\ (kJ/m^2)$
G_{12} = 6	S_{12}= 90	$G_{Ic}^{c} = 79.9\ (kJ/m^2)$
G_{13} = 6	S_{13}= 90	$G_{Ic}^{T} = 0.22\ (kJ/m^2)$
G_{23} =3.7	S_{23}= 40	$G_{Ic}^{T} = 0.70\ (kJ/m^2)$
ρ = 1600 kg/m^3		ρ = 1280 kg/m^3

VI. RESULT AND DISCUSION

During the impact process we can obtain two different output. These are the one which measure the response of structure to impact loading and the other is the one which measure the intensity of damage in the structure. These are the field output and the history outputs respectively. The history output are in the form of central deflection versus time curves, the impact force versus time curves, force versus displacement curves and energy versus time histories curves while the field output are captured in the form of the intralaminar matrix cracking, fiber breakage in both compression and tension modes as well as delamination at the interfaces which is examined in terms of deleted cohesive elements in between two adjacent plies with different orientation. The shape of delamination (peanut shaped) oriented based on the layer just below the interface ply is also observed.

A. History out put

Experimentally the impact force is recorded directly by the load cell yields comprehensive information about the initiation and growth of damage, as well as the stiffness degradation of the composite structure. In addition it also records the history outputs that indicate the laminated plate responses like deflection, force history and the amount of energy absorbed and also other parameters. After the contact between the impactor and the top of plate surface, the plate starts to oscillate and causes a small undulation in time. This undulation can be simulated as deflection versus time curve, which is given as in Fig.3 below.

Table 3: Relation between impact energy, deflection and duration

Energy	Deflection	Duration
7.33 J	6.25 mm	4.60 ms
11.03 J	5.02 mm	5.75 ms
14.67 J	4.0 mm	6.60 ms

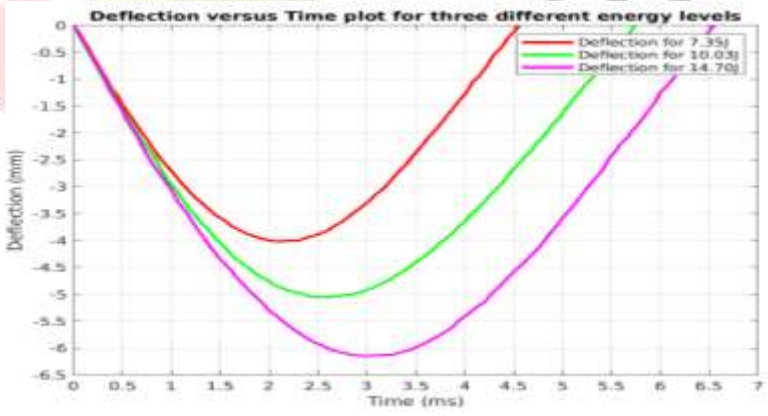

Figure 3: Deflection versus Time plot for three different energy level

As impact energy increase the central deflection of the plate also increase and therefore more damage induce in the structure. From deflection versus time curve we can observe that, as the impact energy increase, both the deflection and the time taken to deflect the plate is increases. The more the deflection, the higher the bending at the bottom ply and result to the tensile failure of both matrix and fiber while compressive failure of fiber and matrix at the top ply of the laminate. Thus the central deflection is a measure of the amount of damage in the laminates. Table 3 shows the relation between impact energy, deflection and duration

This undulation in time versus force curve indicates the initiation or commencement of damage in the plate structure in the form of matrix micro-cracking and interface failure. After this undulation, the time versus force curve reaches to the maximum impact load value known as damage threshold load (DTL), with maximum damage in the form of matrix cracking, fiber breakage, and interface delamination occurring in the plate. After reaching the peak load level (DTL) the time versus force curve starts to drop, which means that the plate is swinging back and the impactor is rebounding. The following force versus time plot of three different impact scenario illustrates the fact. For experimental validation Refer [18]

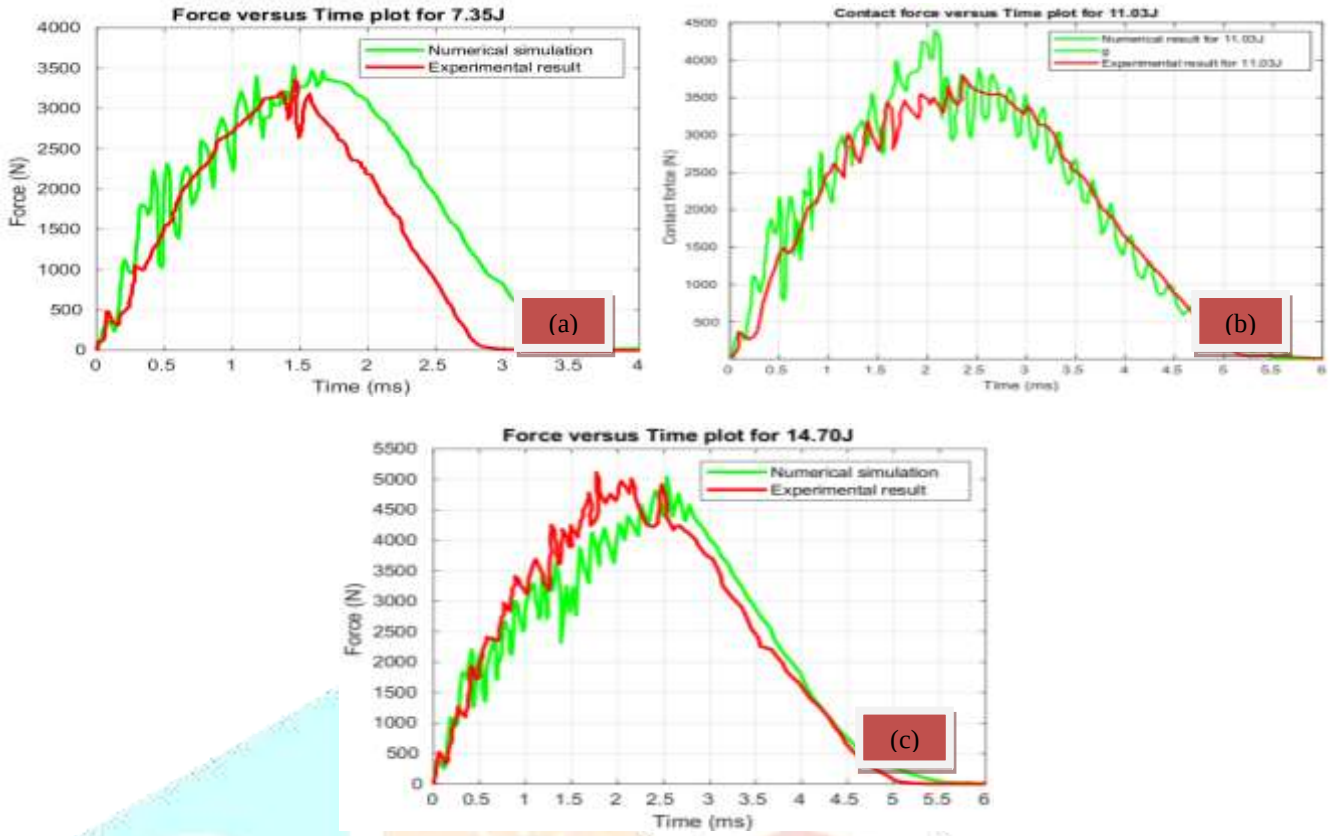

Figure : Force versus Time plot for (a) 7.35J, (b) 10.03J, (c) 14.67 J

The energy absorbed by the plate from the impactor causes the damage mechanisms, and the remaining impact energy is converted in to an elastic deformation or vibration of the plate structure. From time versus energy curve, initially the energy absorbed by the plate is low due to a small amount of damage in the plate. Subsequently the curve rises progressively and reaches to maximum impact energy level; that corresponding to maximum damage to the plate. As the plate starting to swing upward , the time versus energy curve drops to a certain level an becomes straight; indicating that a complete detachment of an impactor from plate surface. If the plate behaves in a complete elastic manner and no damage arises, then all of the impact energy would be converted in to elastic energy or vibration and the energy curve would return to zero position.

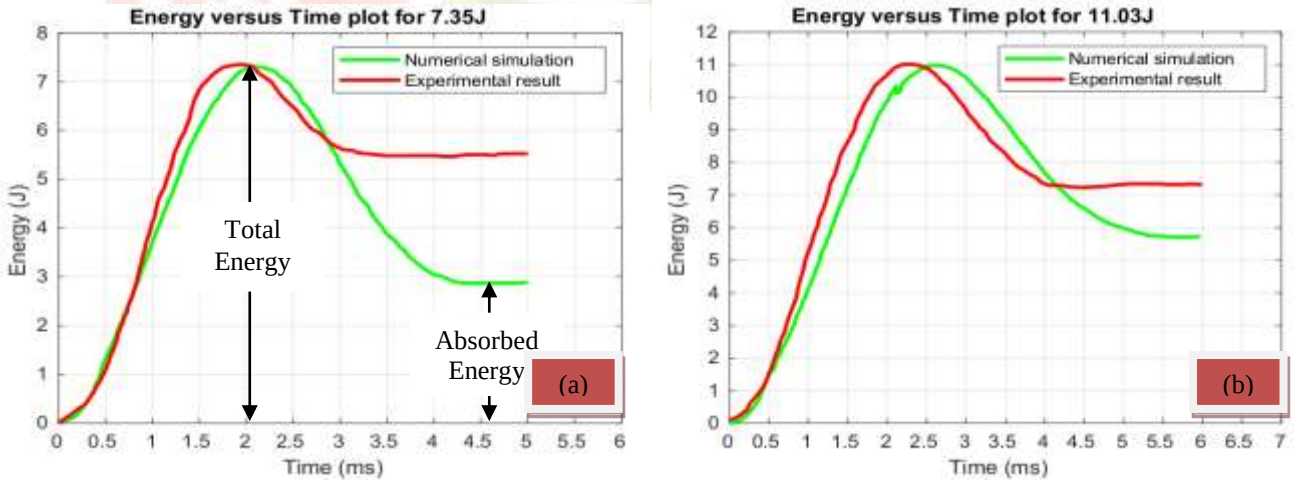

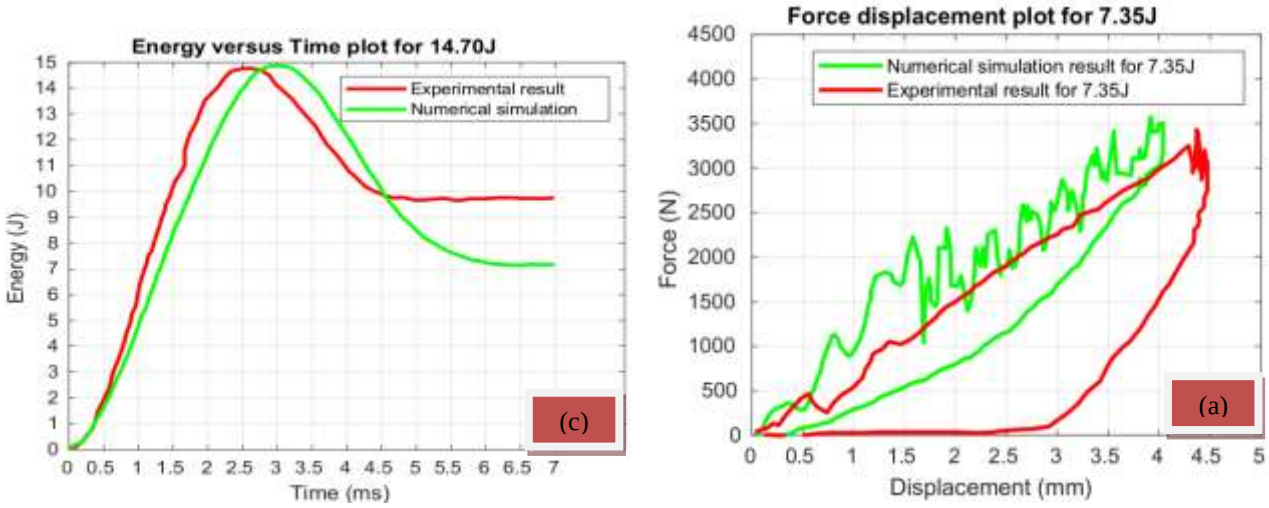

Figure 5: Energy versus Time plot for (a) 7.35J, (b) 10.03J, (c) 14.67 J

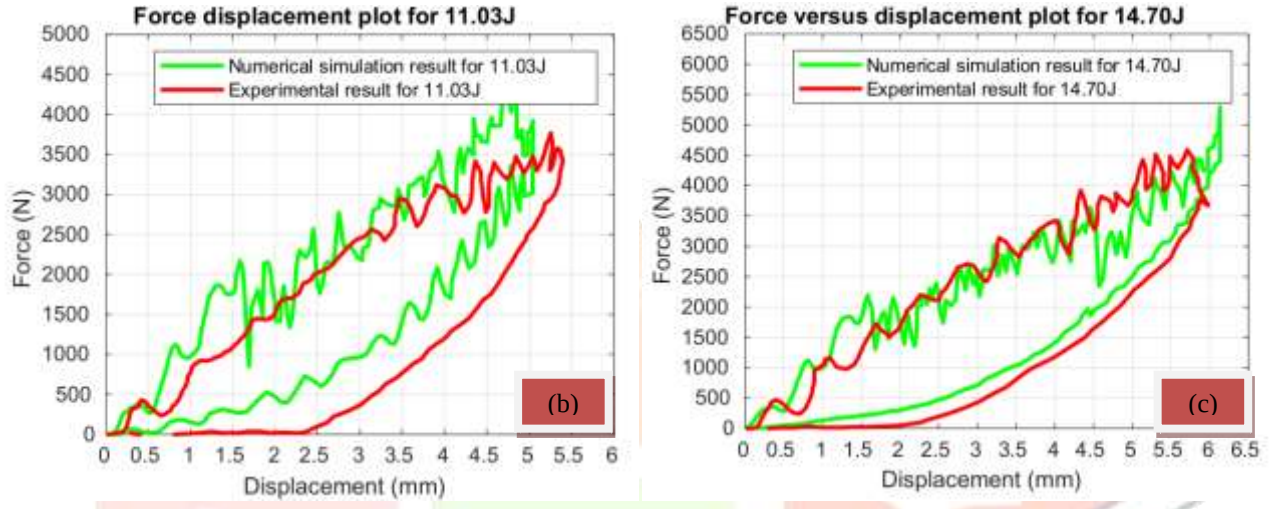

Figure 5: Force versus Diflection plot for (a) 7.35J, (b) 10.03J, (c) 14.67 J

Note that: The Area under force displacement plot implies the amount of energy absorbed during impact process.

B. Field out put

In this paper the field outputs are of two categories. The first one is the output from abacus built-in using continuum shell formulation (SC8R) and the second one is the one obtained from user defined subroutine VUMAT, which is expressed in terms of SDV's with solid element formulation for ply (C3D8R) and cohesive element (COH3D8) for interface elements.

Note that, the higher the impact energy the higher the damage induced in the structure. Therefore, here we are using the out pot of the higher energy level, that is 14.67 Joule. The half cut section is shown here to show the damage at the interior section of the laminate

1. Output from ABAQUS built-in model using SC8R element

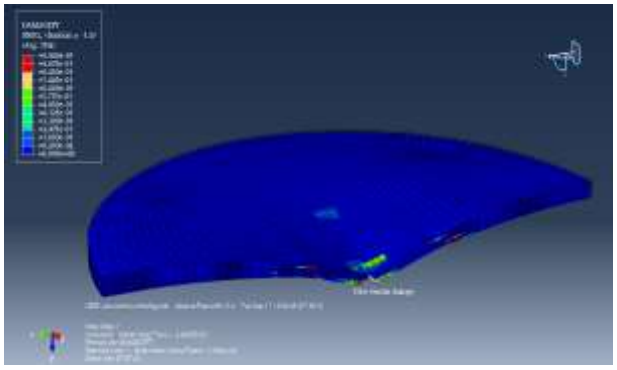

a) Damage of fiber tension (DAMAGEFT)

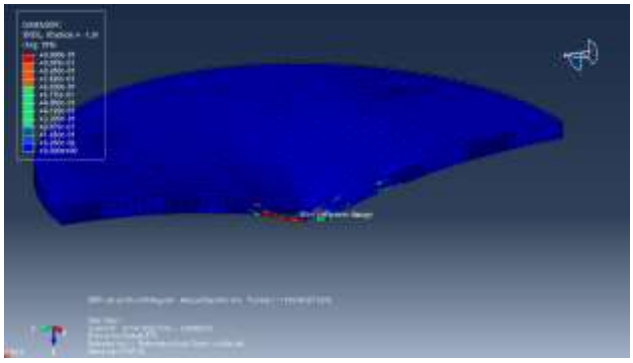

b) Damage of fiber compression (DAMAGEFT)

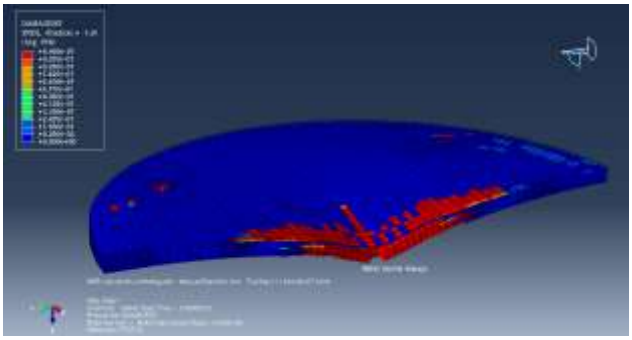

c) Damage of matrix tension (DAMAGEMT)

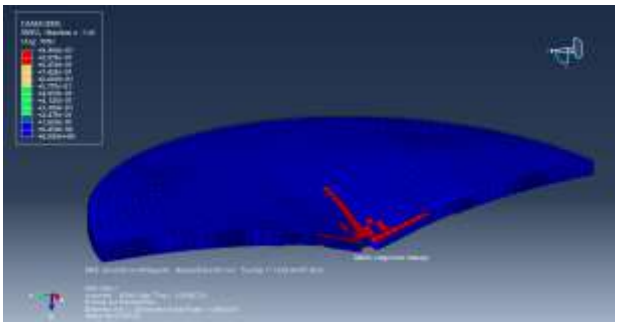

d) Damage matrix compression (DAMAGEMC)

Figure 6: Damage of composite plate impacted with14.67 J using ABAQUS built-in

2. Output from ABAQUS/Explicit VUMAT code using C3D8R elements

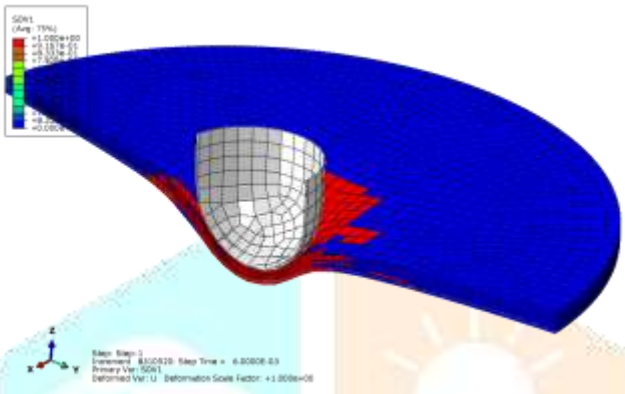

a) SDV1 for 14.70J

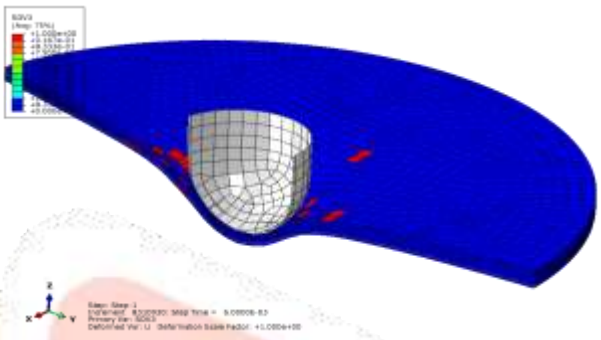

b) SDV 3 for 14.70J

Figure 7: Damage in fiber and matrix using VUMAT

2. Output from ABAQUS/Explicit using COH3D8 elements of Interface damage

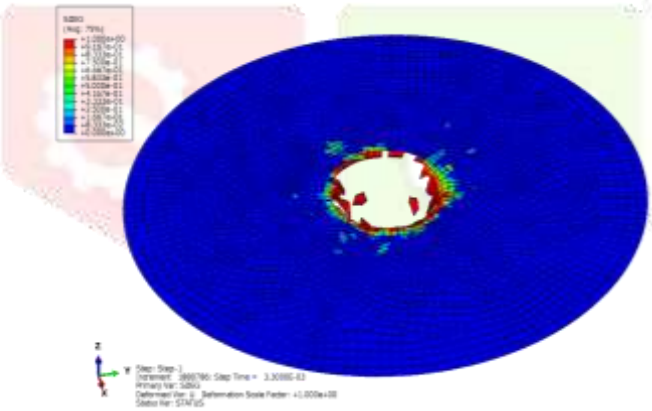

a) Interface 1 (cohesive interface between $0^0/90^0$)

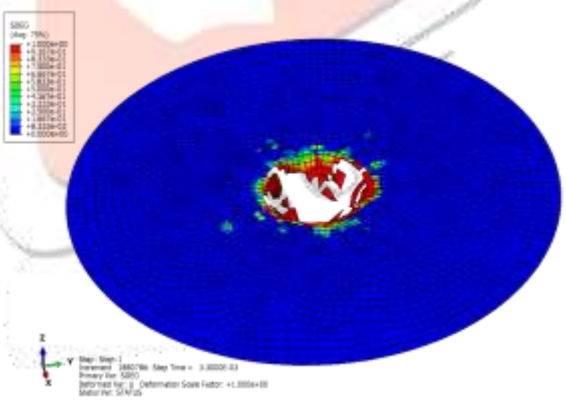

b) Interface 2 (cohesive interface between $90^0/0^0$)

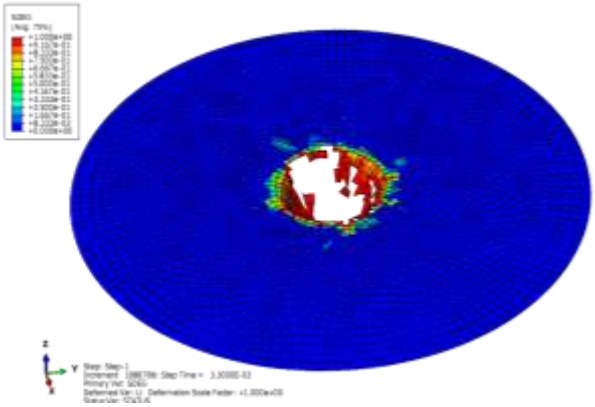

c) Interface 3 (cohesive interface between $0^0/90^0$)

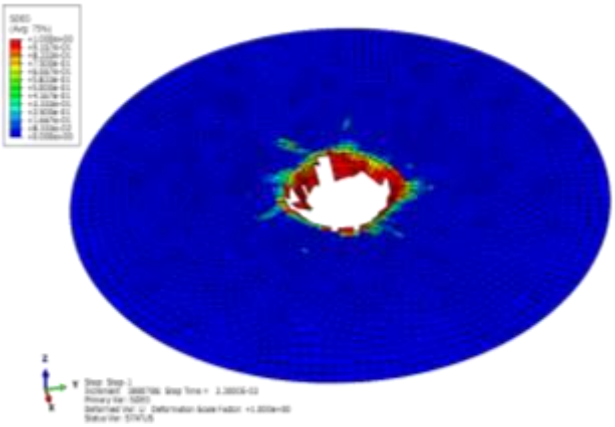

d) Interface 4 (cohesive interface between $90^0/0^0$)

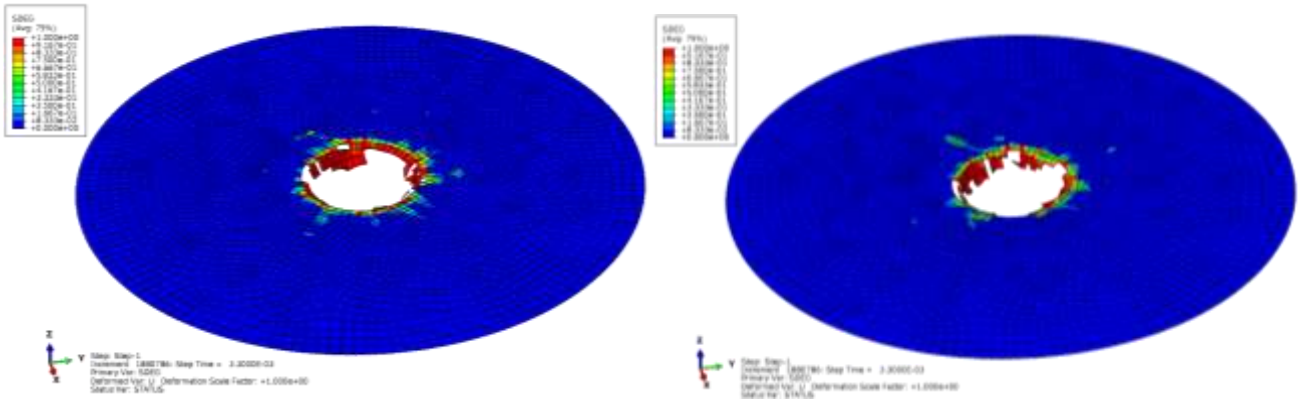

e) Interface 5 (cohesive interface between $0^0/90^0$) f) Interface 6 (cohesive interface between $90^0/0^0$)

Figure 8: The damage of interface element (delamination)

VII. RESULT AND DISCUSION

Three-dimensional solid elements are used to model the unidirectional layers and the Hashin 3D criteria is implemented in *ABAQUS/Explicit* via a user-defined material subroutine (VUMAT) to describe damage and failure initiation of laminate layer. A solid three dimensional cohesive elements are used to model the resin-rich interfaces, and a quadratic stress based damage initiation and mixed-mode fracture energy based damage propagation as (B-K) criteria are adopted to predict delamination at interfaces. The numerical simulation reveals the matrix damage in both tension and compression mode, fiber breakage/failure in both tension and compression and delamination between layers for low energy impact process in the laminate.

The 3D solid model, which includes the through-thickness damage, gives more accurate results than the continuum shell element and the built-in Hashin damage model data. The predicted size and shape of the delamination area show excellent agreement with the drop height impacts test result of different literatures. In addition, the numerical simulation show through-thickness matrix failure in the region directly below the impactor and fiber breakage in the bottom layers of the laminates.

VIII. ACCNOWLEDGMENT

I would like to express my special gratitude to my thesis Guides P.M Mohite (Dr.) and C.S Upadhyay (Dr.) for their wonderful guidance throughout my work. I would also like to thank my lab mate C. Sharat for his valuable help.

REFERENCES

[1] ABAQUS Analysis User's Manual: Volumes I – VI, Version 6.10,
[2] Bouvet C, Castanie B, Bizeul M, et al. Low velocity impact modelling in laminate composite panels with discrete interface elements. Int J Solids Struct 2009; 46(14-15): 2809-21.
[3] Camanho PP, Davila CG, De Moura MF. Numerical simulation of mixed-mode progressive delamination in composite materials. J Compos Mater 2003; 37(16): 1415-38.
[4] Dassault Systèmes Simulia Corp., Providence,RI,2010.
[5] Feng D, Aymerich F. Finite element modelling of damage induced by low-velocity impact on composite laminates. Compos Struct 2014; 108: 161-71.
[6] Hou JP, Petrinic N, Ruiz C, et al. Prediction of impact damage in composite plates. Compos Sci Technol 2000; 60: 273-81.
[7] Liu PF, Gu ZP, Peng XQ, et al. Finite element analysis of the influence of cohesive law parameters on the multiple delamination behaviors of composites under compression. Compos Struct 2015; 131: 975-86.
[8] Long SC, Yao XH, Zhang XQ. Delamination prediction in composite laminates under low-velocity impact. Compos Struct 2015; 132: 290-8.
[9] Lopes CS, Camanho PP, Gurdal Z, et al. Low-velocity impact damage on dispersed stacking sequence laminates. Part II: Numerical simulations. Compo Sci Techn 2009; 69:937-47.
[10] May M. Numerical evaluation of cohesive zone models for modeling impact induced delamination in composite materials. Compos Struct 2015; 133: 16-21.
[11] M.R. Abir , T.E. Tay, M.Ridha, and H.P.Lee. Modelling damage growth in composites subjected to impact and compression after impact. composite struct 2017; 168:13-25
[12] Shi Y, Pinna C, Soutis C. Interface cohesive elements to model matrix crack evolution in composite laminates. Appl Compos Mater 2014; 21(1): 57-70.
[13] Shi Y, Swait T, C. Soutis. Modelling damage evolution in composite laminates subjected to low velocity impact. Compos Struct 2012; 94(9): 2902-13.
[14] Soutis C, Curtis PT. Prediction of the post-impact compressive strength of cfrp laminated composites. Compos Sci Technol 1996;56 (6):677–84.
[15] Ronald K. Virtual crack closure technique: history, approach, and applications. Appl Mech Rev 2004; 57:109-43.
[16] Shi Y, Pinna C, Soutis C. Modelling impact damage in composite laminates: a simulation of intra-and inter-laminar cracking. Compos Struct 2014; 114: 10-9.
[17] A. Version. 6.11. userâAŹs manual. Dassault Systemes 2011;
[18] Y. Shi, T. Swait, C. SoutisModelling damage evolution in composite laminates subjected to low velocity impact Compos Struct, 94 (9) (2012), pp. 2902-2913
[19] James R. Reeder. 2006. 3D Mixed-Mode Delamination Fracture Criteria–An Experimentalist's Perspective, NASA Langley Research Center, Material science 188E, Hampton VA 23681-2199, USA

[20] Gong, X.-J. and M. Benszeggagh. 1995. "Mixed Mode Interlaminar Fracture Toughness of Unidirectional Glass/Epoxy Composite," in Composite Materials: Fatigue and Fracture, Vol. 3, ASTM STP 1230, R.H. Martin, Ed. ASTM Int., W. Conshohocken, PA. pp. 100-123.